

Designing a Uniform Magnetic Field to Detect the Electric Dipole Moment of a Neutron

Christopher Ian Delcher

August 11, 2022

1 Introduction

The breaking of symmetries, particularly charge conjugation (C) and charge-parity symmetries (CP), in particle systems are essential in uncovering the secrets of the early universe. Evidence against C and CP (and thus Time symmetry) invariance may help explain the abundance of matter over antimatter, or the Baryonic Asymmetry of the Universe. If these symmetries were truly invariant, theoretically, there should exist equal amounts of both types of matter (as Andrei Sakharov realized), contrary to what modern measurements are telling us. Physicists are searching for more evidence of these symmetry violations that could lead to an explanation to the aforementioned phenomena [1].

A promising piece of evidence, if can be proven with the development of an extremely uniform magnetic field, would be the electric dipole moment of a neutron (nEDM). The dipole moment results from a subtle separation of the quarks in a neutron, similar to the way a molecule is polarized with partial positive and negative charges. These weak interaction within quarks are theorized to break CP symmetry. Evidence of a non-zero nEDM violates both Parity and Time symmetries [1]. The separation of these quarks behaves differently in a mirror-reflected world, or Parity symmetry, as well as in one where time is reversed. As my teammate Stephanie Betancourt denotes, this is evident in the equation $d_n = \vec{d} \cdot \vec{\sigma} = q\vec{r} \cdot \vec{r}' \times m \frac{d\vec{r}'}{dt}$. Parity symmetry is violated when $P : \vec{r} \rightarrow -\vec{r}$, so d_n is also reversed. Time invariance is also violated because $T : t \rightarrow -t$, so d_n , the observable EDM range of frequency, becomes reversed as well. \vec{d} is the EDM vector that is not measured. $\vec{\sigma}$ represents the spin or angular momentum of the neutron. In $q\vec{r}$ q is the charge of quarks and \vec{r}' presents the level of separation in respect to the center. Lastly, $m \frac{d\vec{r}'}{dt} = P$ where P is momentum. These inconsistencies make the nEDM a potential piece of insight to the antimatter-matter issue.

Because the nEDM would be magnitudes of times smaller than the tiny neutron itself, a uniform magnetic field is imperative to highlight any possible resulting disturbances in the field. Even an extremely minuscule difference of 1 fT in a less uniform field can imitate the signal for a non zero nEDM [1].

Therefore, the design of these types of magnetic fields is one of the most important aspects in the search for an nEDM. However, this type of testing would be severely limited with the electromagnet currently designed [3]. Our project seeks to improve upon this previous electromagnet and test the magnetic fields associated with our designs so that they can be effective in future nEDM detection experiments.

2 Procedure Overview

Our research is composed of two main parts. The first is to develop a design through computer-aided design (CAD) to improve upon a faulty design of the electromagnetic coils. The second part is testing, mapping, and comparing the strengths of the magnetic fields of multiple coils.

2.1 CAD Implementations

The electromagnet has an sturdy aluminum skeleton, which a resin-printed "skin" envelops. The previous model, which uses only grooves to hold the wire in place, does not do its job ably [3]. This results in a much less uniform magnetic field compared to when the wires are tightly secured in a confined space. We have redesigned a coil clip design and have implemented this refurbished design with the preferred blueprint of the magnet that will be used in experiments [3]. Fusion 360 was used to produce testable prints for the aluminum skeleton.

2.2 Testing and Mapping the Magnetic Field

In a nutshell, to detect a nEDM of 10^{-23} cm we would need a magnet with a level of uniformity of

$$\frac{\Delta B}{|B|} = \frac{10^{-7}}{cm}$$

where B is the magnitude of the magnetic field [2] This should be taken into account in testing and mapping of the final magnet using the robotic mapper and top-level multiphysics softwares. Before testing the real double cosine theta magnet, we produced simulations of single cos-theta and saddle coils—the latter is less relevant but still applicable to differences in winding methods—to understand how the B-Fields can be calculated in practice. Understanding these basic methods will assist in mapping the uniformity of the final magnet and will further allow ease of understanding what adjustments need to be made when the final magnet is tested with more advanced technologies.

To mimic the geometry of the double cos theta coil that will be used for measuring the nEDM, copper wire was wound around non-conducting skeletons of various sizes in single-cosine theta form. Each point at which the coil sharply curves upwards or downwards along the cylinder was mapped as a coordinate point using trigonometry (hence, cos-theta). Since all designs will be cylindrical, the points can be mapped in respect to the center of the cross-section at the

very bottom of the shape ($x = 0, y = 0, z = 0$). Given a previously developed script in MATLAB, we then input these points as arguments in a function to find the strength of the B field at a given point on the cos theta coil. The wires should be wound along the equipotential lines of the magnetic fields to produce the expected B field in the equation, which can be calculated with a magnetic scalar potential equation [2]. These lines can also be visualized geometrically after abstracting the mathematics away (see Section 5). The theoretical field strength values were compared with the experimental value measured using a magnetometer. Very similar methods were also used for the saddle coil; mapping procedures for both types of coils are discussed further in Section 6. By constantly testing and comparing, an optimal structure for the winding of the coils around the final magnet can be determined.

3 CAD Components for Electromagnets

A critical element of the process in building and testing electromagnets to assist in detecting the nEDM is knowing how to use CAD software. Popular applications include Autodesk Fusion 360 or Autodesk Inventor Pro. 3D resin design were printed using the former. Though these designs were printed to fit the exact dimensions of the aluminum skeleton provided, the basic functions of the designs can be applied to any shape or type of electromagnet and wire.

For the aluminum cylinder, the designs include four outer "skins" that fit the curvature of the skeleton and completely cover it. On the skins lie the clips for the wires. The clips consist of a rectangular base that has a curvature on which the wire lies (also known as the "trench") as well as two lips that curve a top the wire to keep it in place.

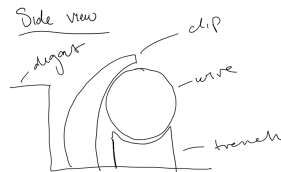


Figure 1: Clip Design: From Left to Right: Digout, Clip, Trench with 24 Gauge Wire

The dimensions of the clips vary based on the gauge of the wire. Dimensions for 20 Gauge and 24 Gauge wire were calculated to be 0.34 mm and 0.55 mm in diameter, respectively. The designs for the trench accounted for the size of the wire and were adjusted to have a larger curvature than the cross section of the wire given its diameter. This is simply to allow for it to rest comfortably on the trench. On the contrary, the two clips (only one is shown in Figure 1) were placed at a distance from each other that is *less* than the length of the diameter. This is so that the wire is securely held in place. If the distance was the same

or greater than the wire's diameter, the wires would fall out of place. Given this, the base of each lip clip must be thin enough to offer enough flexibility to have the clip move from its fixed position to allow the wire to enter. The exact curvature of the clips are negligible, however the spacing between two clips in around the trench is not. We found that the 24 gauge wire was not staying in the clips on the first print. On the second print, the clips were pushed together by a constant amount, and the wires secured in nicely. These exact spacings vary based on the capabilities of printers and the size of the wires.

The clips were tested by printing a singular skin of the cylinder with multiple clip designs added onto its surface. These were parallel to each other with an equal spacing in between each of the clips in order to best mock the actual winding conditions. One problem that was encountered when clipping in the wires was that the copper would bend under the pressure of winding. This excess curvature would create multiple rogue dipoles that would affect the uniformity of the field, despite the wire being securely clipped. A solution was found by applying the pressure on the wire directly above the clip itself and not in between the clips. If the point on the clip design where the force is applied to the wire is consistent throughout the winding, then the wire will not curve under uneven pressures.

Once all of the clip components were measured, printed, and tested, they were added onto the skins for the aluminum cylinder through Fusion. Once one complete skin included with the clips on the surface was fully designed, four were printed to cover the skeleton. The more difficult element of the CAD design was designing a lip to act as a bridge from the outer skins to the inner skins of the skeleton. This included determining equipotential paths to wind wire and place clips along.

4 Winding a Double Cosine Theta Coil Along Equipotential Lines

The winding of the double cos-theta coil for nEDM experiments and research does not follow the perfect rectangular geometry of the traditional cos-theta coil (discussed in Section 7). This type of cos-theta coil winding and turning points along the structure of the magnet follow the double cosine theta distributions and, along with some additional top-level math, help determine the winding paths along the equipotential lines of the magnetic field. The locations of these winding paths can be output by programming in COSMOL Multiphysics Software [4]. The data analytical software ROOT, developed by CERN can also implement the Biot-Savart formula to calculate the B-Field produced by the current at any point [4]. These two softwares, along with similar ones, can allow us to judge the uniformity of the wound double cosine-theta in our research and to make adjustments. The winding of wires along the equipotentials of a *double* cosine theta coil ensures a constant field on the inside and zero field on the outside of the magnet. In a nutshell, one element of the double cosine theta

coil generates the B-Field within the cylinder while another element redirects the fringe fields created by the first part back into the magnet. The magnet's resulting coils follow a more curved path along these lines and around the magnet in comparison to the single cosine theta coil's rectangular winding paths in order to provide (or eliminate) fields in certain places.

4.1 Determining Equipotential Lines

After abstracting away all of the top level math that allows for this, the equipotential lines' paths can be much more easily described for a double cosine-theta. These paths can be found geometrically by splitting the inner circle of the cylinder with equally spaced lines. A cylinder with the exact dimensions of the aluminum skeleton with the skins included was used in Fusion for mapping these lines. The number of lines used to split is directly proportional to the number of coils the electromagnet would have. Basing the number of coils for the final electromagnet on the number of coils in the previous faulty design, the aluminum skeleton's inner circle was split with 38 lines across its area in CAD. Once the face had been divided, a point was noted exactly in the middle of two lines on the edge of the inner circle face for every two lines drawn. Finally, a three-point arc was drawn that connected the center of the circle face with one of these points on the top half and its parallel point on the bottom half. After this was done with all the points, the design resembled familiar magnetic field lines.

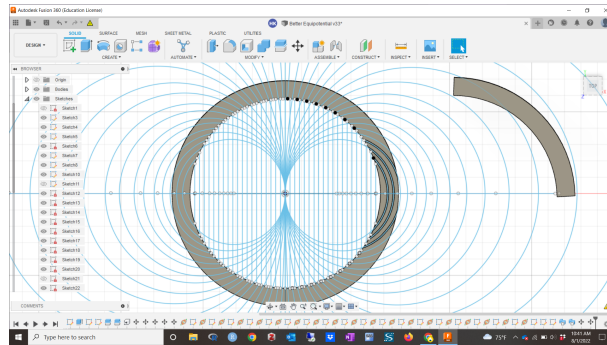


Figure 2: Equipotential paths can be determined by splitting the circle into sections and drawing three-point arcs from the center to points in the middle of each of the lines.

There are 19 rings on each half of the cylinder. Where each of three-point arcs cross the width of the aluminum skeleton are where the equipotential lines for this double cosine theta coil with 38 coils are located. The equipotential lines continue downwards along the length of the aluminum cylinder until the wires reach the bottom circular face. This face has identical equipotential paths of the first face. The clips from the clip designs were placed along these paths in order to wind wire along these lines.

4.2 Equipotential Lines on Lips Using CAD

In Fusion 360, the clip design for the wires were isolated in order to be placed along the equipotential lines displayed by this three-point arc method. First the cylinder was "de-extruded" to a width of about 2 mm. This was then split up into fourths, aligned, and fused with the skin design as the lip since the skins are about a fourth of the circumference of the outer circle of the cylinder. We altered these paths to make "troughs" in the surface of the lip. The singular clip components of the entire clip design were taken from the design to be placed around each of the trenches. This was simpler than trying to bend the entire clip design around a curvature. When the isolated clips met the edge of the lip, the *entire* clip design was continued on a vertical line downwards along the skin's length after the lip design and the fourth skins were fused together in the software. For simplicity, only two fourths of the whole lip body needed to be designed with the clips since there exists rotational symmetry along the circle face (within the capabilities of fusion). At this point, the magnet could be prepared to be wound and tested in MATLAB.

5 B-Field Mapping Simulation Set Up

Before mapping the b-field vectors and strength using the completed magnet, we found it best to be acquainted with the experiment process through running a simulation. For our simulation of the B-field vector mapping, we wound an already-printed resin cylinder with grooves along the sides in the form of a single cos-theta coil (winding discussed in Section 7.1). For measuring the strength of

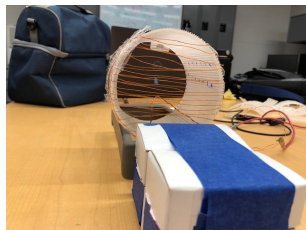


Figure 3: Cos-Theta Coil: Simulation Set Up

the field for the simulation, an application called Physics Toolbox Magnetometer was installed on my teammate's cellphone, which reads changes in the B-Field relative to the defined axes on the phone. The measurements are taken at every millisecond and are very precise for a mobile application. Since this was only a simulation of the final project, we accepted the experimental error that this measuring device brought.

5.1 Measuring With Axes

Placed on its side with its circular plane facing towards us, the dimensions of the cylinder can be defined by the three axes x , y , and z . In respect to this configuration of the coil's circular face, the plane across it (horizontally) corresponds to the x axis, the vertical plane to the z axis, and the plane perpendicular to the circular face going into the cylinder is the y axis.

The z axis was split up into designated points of low, medium, and high heights relative to the bottom of the cylinder. These conventions were given the values -1 , 0 , and 1 , respectively, which are equally spaced out to an inch. The magnetometer was then aligned with these values by placing the cell phone on top of small boxes one inch in width as shown in Figure 3 (one box for -1 , two boxes for 0 , and three boxes for 1).

The y axis – the plane going into the cylinder – was split into increments of $1/2$ inch along the inner side of the cylinder. The cell phone's magnetometer was carefully placed at these y -points using a crude measurement device as shown in Figure 4. The cell phone's built-in magnetometer at the top of the cell phone

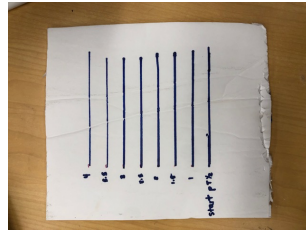


Figure 4: Incremental Measurements for Y Points; Split Into Increments of $1/2$ Inch

reader would be y inches into the cylinder when the bottom of the phone was at the y mark on the measuring device.

Finally, the x axis was separated into qualitative conventions, with the magnetometer sensor either to the far left, far right, or exactly in the middle in respect to the center of the circular face. These conventions have negligible numerical values and allow for simplicity when noting point locations. With these values defined at each of the axes, we began plotting points and gathering data for the B-Field strength calculations at every combination of x , y , and z that was defined. Each of the conventions used for the points are for readability and simplicity when entering the measurements into a script in MATLAB or an Excel Spreadsheet.

5.2 Gathering Data

Using the right hand rule, and given the orientation of the electromagnet as shown in Figure 3, the B-field vector traveled vertically, pointing downwards. The cell phone's magnetometer was placed into the magnet, perpendicular to

the B-Field vector, at each of the defined points inside the coil. For example, the magnetometer would read all the y points along the inside of the coil at $z = -1$, and at the x point corresponding the far right (x known by its corresponding numerical value). It would continue measuring each of the y points along the inside for each combination of x and z.

The Physics Toolbox Magnetometer application has a built-in function that recorded the data for the b-field strength at the axes of the phone for five seconds. The app then put this data into a document that was edited (Note: the phone's axes are *not* the same as the axes of the coil; we'll call the phone axes b_x , b_y and b_z). These values of b_x , b_y , and b_z collected for five seconds were the field strength data for *one* point on the axes of the cylinder. Since the magnetometer detected in increments of 1 millisecond, the abundance of b_x , b_y , b_z data points in the five-second reading were each organized and averaged in an Excel Spreadsheet. The process was repeated for all points defined.

The averages b_x , b_y , and b_z data for each point in the cylindrical coil were categorized in the spreadsheet by z point first, then by x point, then finally by y point. Once the data had been gathered, it was entered as arguments into a script in MATLAB to get a visualization of the experimental data that could be compared with a theoretical visualization of the B-Field vectors.

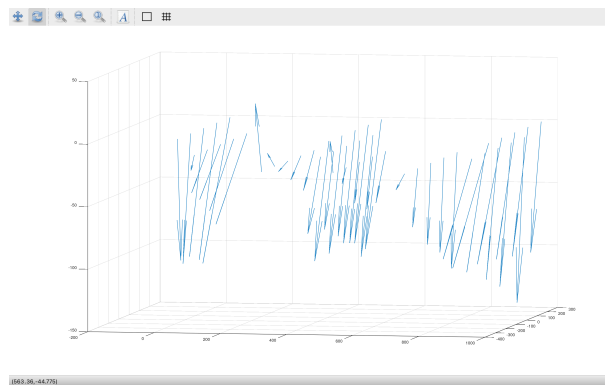


Figure 5: B-Field Vector Visualization for Cos-Theta Simulation

If the field was uniform, then vectors (arrows) would be pointing directly downwards. Here, some of the arrows are skewed, indicated that the field is not uniform. This makes sense due to the large margin of error in using a roughly wound coil and a cell phone application. These types of graphs represent data in a way that is very easy to understand and to make adjustments to the magnets that are being tested.

6 Conclusions

Developing a working prototype of an electromagnet for nEDM experiments is extremely important in order to implement these certain procedures and techniques to the actual magnets used to test this in the experimentation phases. If a non-zero nEDM is detected in one of these magnets, there would be evidence for CP, C, and T symmetry violations. Observing these types of symmetry violations would give much insight to the Baryon Asymmetry, which could reshape the Standard Model and support several theories such as supersymmetry. In order to do this however, neutrons must first be passed through an extremely uniform magnetic field for any possible detection.

6.1 Overview

6.1.1 CAD

The uniform magnetic field prototype for nEDM experiments has had previous designs. One of them included printed cylinder with grooves along the equipotential lines where wires would fit. However, this design was a faulty one because the wires would not stay in place very well, which significantly affects the uniformity of the field.

A new design was thought of which included the aluminum skeleton with holes drilled into the sides where pegs on the back of skins would fit into. This skin and peg design fit the aluminum skeleton's curvature very well and required significant effort to remove from the skeleton once it was placed in.

A previous design for the clips was also made, however it was complicated and too small for any type of wire. It was not efficient to wind with, so the design was replaced with the design shown in Figure 1.

In order to wind over the top of the magnet correctly, equipotential paths were drawn over a lip with clips surrounding the paths. The skins and the clips were fused together, with the clips placed on the curvature of the skins as a continuation of the equipotential paths downwards. The lips were fused with the top and the bottom of each skin. Two skins, each with two different rotationally asymmetric lips, effectively fit around the skeleton.

Due to the inevitable error that the printer brought with each production of the CAD designs, it is important to print them at highest resolution possible, especially if design components are particularly small. This is because the printer neglects designs that are below a certain size threshold when printed at the default resolution.

6.1.2 Magnetic Field Mapping

Along with designing an optimal structure for a uniform electromagnet, multiple simulations were run where different types of coils were charged with current and had their resulting b-fields calculated. A significant simulation was that of the single cosine theta coil. Points were defined in respect to the axes of the

cylinder. Using a magnetometer on a mobile application, magnetic field data was measured at every point defined and organized into an excel spreadsheet.

This data was then entered into a script in MATLAB developed by Dr. Christopher Crawford to generate visualizations of the B-Field vectors. These visualizations make it convenient to see how uniform the magnetic field is helps in making adjustments to the designs to improve upon the data.

6.2 Next Steps

6.2.1 Inner Skins and Adjustments

The nEDM electromagnet prototype outer skins were finalized and completed over the course of this research, but due to time constraints, the inner skins were left incomplete. Through testing the current designs for the inner skins around the inside of the aluminum skeleton, it is evident that the curvature does not match that of the skeleton. This results in an uneven surface between two skins side by side because they are too wide and they overlap. The distance from the top of the inner skin may need to be adjusted to exactly meet the edge of the lip on the outer skins as well. Once these elements of the inner skins are fixed, clips can be placed as continuations of the equipotential lines in a similar fashion as was done the outer skins.

We also found that the addition of the singular clips, separate from the entire clip design, onto the lip design was ineffective in keeping the wires in place here. The isolated clips were more fragile, and there was increased room between the surface of the lip and the clips due to the troughs created by the "sweeping" function. A more effective method may be to curve the entire clip design along the equipotential paths; the full clips effectively keep the 24-gauge wire in place.

Exploring the abilities of Fusion 360 helps immensely to the progress of this research and contributes to its efficiency. Placing the clips on the curvature of the skin is a good example of where this knowledge should have been applied. Because the skin was not level in the design relative to the plane it sat on by the slightest millimeter, the vector along the length of the skin was at an angle to the y axis of the workspace. Thus, when the clips were copied, pasted and translated downwards in a straight line, the result was uneven relative to the skin. Parts of the clip were inside the body of the skin while others were not touching it at all. Fixing this issue is time consuming and so is placing the clips on the skin free-handedly in Fusion 360. It would be much easier to produce these types of prints if there were a function that automatically translates the base of the clips onto a curved surface, or something similar. A more experienced researcher in Fusion 360 may be able to find a solution and improve the accuracy of the distribution of clips along this face of the cylinder.

6.2.2 Mapping the Final Electromagnet Prototype

Due to the incomplete final magnet, the B-Field vectors were not mapped with the robotic mapper in the lab, nor were they visualized using MATLAB and the

techniques explored in the simulation. After completing the CAD components of the prototype, the magnet should be wound and tested with this B-Field mapper. The MATLAB visualizations also add to understanding how uniform the field is compared to

$$\frac{\Delta B}{|B|} = \frac{10^{-7}}{cm}$$

which is the level of field uniformity needed to detect a nEDM of 10^{-23} cm [2]. The CAD designs around the aluminum skeleton should be adjusted accordingly until the measurements and readings indicate a favorable uniformity before finalizing the electromagnet prototype.

7 Additional Electromagnet Winding Methods

An electromagnet's effects are dependent on the way the wires are wound around it. Each type of winding serves for different kinds of experiments concerning electricity and magnetism. In this section, a couple of different winding methods that could be helpful nEDM applications will be discussed.

7.1 Cosine Theta

The cos-theta coil is the type of coil that was wound in the simulation of the b-field vector mapping. The coils of this winding method are rectangular instead of circular. Before beginning, an extension of wire was allowed for slack and ease of winding. We started by winding a copper wire along the geometry of a cylinder so that the wire began at one of the circular faces, passed the other face above it and came back, passing the same circular face from where it started. Once the wire reaches its origin point on the way back, the wire must be secured in some way. In the simulation, tape was used. This completes the winding of one coil, and its rectangular shape should be perpendicular to the circular faces. This process should be repeated along the magnet – shifting a constant lateral distance for each coil – for however many coils will be wound. It is important that each of the coils are equally spaced apart.

The turning points of each coil – the "corners" of the rectangle of wire – created their own fringe fields, or rogue-dipoles. These fringe fields along the bottom of the cylinder could affect magnetometer readings in general, so they were canceled out. To do this, we brought the remaining wire after finishing the winding along each of the turning points of the coils at the bottom of the cylinder. This canceled out any lingering dipoles there. The extension of wire at the end of the winding also met with the extension of wire at the beginning (the slack), which we crossed over one another in a braiding fashion. This also eliminated any fringe fields produced by these wires and finalized the winding of the single cos-theta electromagnet.

7.2 Saddle Coil

Another important winding method to implement in electricity and magnetism research is that of the saddle coil. The saddle coil's design differs from the cos-theta coil in that the "rectangular" coils of the saddle design are wound along the inside of the cylinder in a warped, saddle-shaped way (hence the name). Half of the coils were wound on one hemisphere of the inside of the cylinder and the other half of the coils were wound along the other hemisphere. The winding method for the coils included pegs on which the wires would loop around. The photo below also shows the quadrants of which the pegs are divided into.

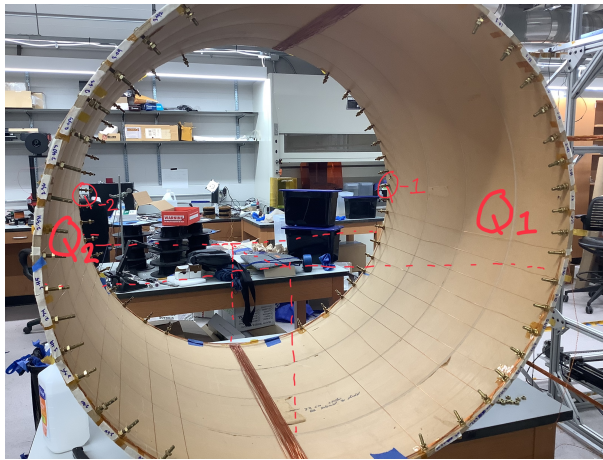


Figure 6: To the right: Quadrants 1/-1 To the left: Quadrants 2/-2

A problem that arose from these winding aides was the unintentional creation of dipoles. As a wire wound around one of the pegs, either under or over it, a tiny dipole was produced. There is no way to prevent the creation of these while still using the peg method for winding the saddle coil. Yet, the fringe fields can still be balanced or canceled out as they were in the cos-theta coil.

Winding began at the middle peg at the horizontal diameter of the circular face of the cylinder in Quadrant 1. The wire went under the first peg, then over the next one, and alternated until the bottom peg of Quadrant 1 was reached. Because of the alternating winding directions over each peg, opposite-facing dipoles were produced and canceled each other out. There existed an *even* amount of pegs on each quarter of the face for a complete cancellation.

Once this was done, the wire was brought along the inside of the cylinder to the bottom peg on Quadrant -1. The wire was wound over this peg, then brought to and wound over the peg parallel to it on Quadrant -2. After it was wound over this peg, the wire was brought over the peg on Quadrant 2. From this peg, the wire was brought back *under* the Q1 starting peg to cancel the "over" winding of the Q1 bottom peg at the beginning. This completed one coil.

When the next coil was started, the wire was brought up over the second peg in Q1 and along the inside of the cylinder, following the same path to the second peg in Q-1. It went over this peg and under the peg below, following the alternate winding pattern to cancel out the "over" winding from the first coil. The same general pattern was followed, but that the wire was wound around the opposite way of each peg from the peg before it.

If this pattern of alternate threading is consistent during the winding of all of the pegs for a the saddle coil, then all of the dipoles would cancel out. Also, it is important that once all of the coils are wound the diameter pegs for the first half of the cylinder, this loop should be terminated and a new, similar loop must be wound in the same way for the second half of the pegs on the cylinder. We found that, in the case of having to flip over the magnet for ease of winding the second hemisphere, the winding directions and alternating patterns will all be flipped and opposite.

Once winding for both hemispheres is complete, the excess of wire in the beginning of winding and at the end of winding should meet up in the way discussed in Section 7.1 The saddle coil can then be finalized.

8 References

- [1] Crawford, C. "Robotic Mapping of Magnetic Fields in a Magnetically Shielded Environment". In: KY NSF EPSCoR PROJECT DESCRIPTION.
- [2] Hunter, B. Spencer, L. K. and Crawford, C. "Drilling a double cosine – theta coil". In: University of Kentucky poster presentation.
- [3] Ziemyte, G. "Designing and Winding an Electromagnetic Coil". In: REU Project Proposal
- [4] Martin, E. and Crawford, C. "A Double Cosine Theta Coil Prototype". In: University of Kentucky research paper.